Adducts of Antimony(V) Pentachloride with Neutral Lewis Bases. Part I. Structure and Stability: a Vibrational and NMR Study*

JEAN-ETIENNE KESSLER, CHRISTOPHER T. G. KNIGHT** and ANDRÉ E. MERBACH†

Institut de Chimie Minérale et Analytique, Université de Lausanne, Place du Château 3, CH-1005 Lausanne, Switzerland

Received October 24, 1985

Abstract

A large number of $SbCl_5 \cdot L$ adducts were synthesized (L = RCN, $R_{3-n}R'_nPO$, ethers and various other oxygen donors). The adducts can be assigned to the C_{4v} point group according to the infrared and Raman spectra of both the solids and the solutions in dibromethane. Antimony-121 NMR was used to monitor the extent of auto-ionisation due to reaction: $2SbCl_5 \cdot L \rightleftharpoons SbCl_4 \cdot 2L^+ + SbCl_6^-$. This increases with the polarity of the solvent and the donor strength of the ligand, but was always less than 3%. ^1H and $^{13}C\{^1H\}$ NMR were used to establish the relative stability constants of the series of adducts in dichloromethane. A linear correlation of slope near unity is observed between the relative free energy of formation and Gutmann's donor number. A correlation is found between the adduct stabilities and the various metal–chloride stretching frequencies.

Introduction≠

Although considerable information now exists concerning the mechanisms of ligand substitution reactions on octahedral coordination compounds [1], there is little knowledge available for labile reaction centers involving high oxydation state metals. In order to rationalise their mechanisms, we have undertaken an extensive study [2–4] of the exchange reactions of adducts of metal halides with Lewis bases in inert solvents, as described in eqn. (1).

$$MX_{6-n} \cdot nL + {}^*L \rightleftharpoons MX_{6-n} \cdot (n-1)L^*L + L \qquad (1)$$

This type of reaction provides an appropriate basis for systematic study since it is common to a large number of transition metals, it is simple and proceeds almost always by a single step.

We now wish to report the results of our study of the adducts of antimony(V) pentachloride with a series of neutral Lewis bases. In this paper, we deal with the preparation of the $SbCl_5 \cdot L$ adducts and their infra-red and Raman analysis both in the solid and in solution. The relative stability constants of the adducts have been obtained by NMR and are discussed in the light of both the donor-number, DN, of the ligand as proposed by Gutmann [5], and the metal–chloride stretching data. This provides the necessary background for the mechanistic study of the fast Lewis base exchange reactions of $SbCl_5 \cdot L$ adducts as reported in the following paper.

Experimental

Sample Preparation

Since $SbCl_5$ and its' adducts are prone to hydrolysis on contact with atmospheric water, all preparations were undertaken in an inert N_2 atmosphere (water concentration of less than 2 ppm). $SbCl_5$ (ROC/RIC 99.99%) was stored under N_2 and used without further purification. The various Lewis bases and solvents required were dried and distilled using standard methods, and stored under N_2 over molecular sieves where necessary.

Solid adducts were prepared by adding the appropriate quantitites of $SbCl_5$ and Lewis base to the solvent (usually CH_2Cl_2) and either directly evaporating to dryness, or forcing crystallisation by the addition of n-pentane and filtering the resultant mixture. In both cases the products were dried over KOH at 5×10^{-2} Torr, then sealed in Pyrex tubes under vacuum. Representative samples were immediately dispatched for elemental microanalysis to A. Bernhardt, 5251-Elbach, F.R.G. In all cases, the results were in excellent agreement with the given formulae.

*Taken, in part, from the *Ph.D. Thesis* of J.E.K.

**Present address: School of Chemical Sciences, University of Illinois at Urbana-Champaign, 505 South Mathews Avenue, Urbana, Ill. 61801, U.S.A.

†Author to whom correspondence should be addressed.

≠Abbreviations: tetrahydrofuran = THF, dimethylsulphoxide = DMSO, dimethylformamide = DMF, dimethylacetamide = DMA, tetramethylurea = TMU.

0020-1693/86/$3.50

© Elsevier Sequoia/Printed in Switzerland

The $SbCl_5 \cdot L$ solutions were prepared by mixing the appropriate quantities of $SbCl_5$ and Lewis base (as 10% or 20% *w/w* solutions) with the desired solvent (CH_2Br_2 for samples destined for vibrational studies, and mixtures of normal and deuterated dichloromethane or chloroform for those used for the NMR measurements). Solutions were prepared to have a final concentration of $SbCl_5$ of 0.1 to 0.3 m (m = mol kg^{-1}) and a [$SbCl_5$]:[ligand] ratio of 1:2.

Vibrational Spectroscopy

Raman spectra were recorded between 600 and 50 cm^{-1} on a SPEX 1403 spectrometer using an argon or krypton laser. Samples were contained in capillary tubes. Between 100 mW and 500 mW of power was used, depending on sample stability.

Infra-red spectra were recorded between 650 and 140 cm^{-1} on a Bruker IFS 113-C Fourier Transform spectrometer. Solid adducts were prepared as Nujol mulls and placed between polyethylene windows.

NMR Spectroscopy

The spectra were obtained using Bruker WP-60, CXP-200 and WH-360 Fourier Transform NMR spectrometers, operating at 1.4, 4.7 and 8.5 T, respectively. For ^1H, the spectra were recorded over a sweep width of 720 Hz (90° pulse width = 2.5 μs) at 60 MHz. $^{13}C\{^1H\}$ spectra were recorded at 50.3 MHz over a 2 kHz sweep width (90° = 24 μs) and at 90.55 MHz with an 8.9 kHz sweep width (90° = 14 μs). $^{31}P\{^1H\}$ spectra were recorded at 24.3 MHz over a sweep width of 16 kHz (90° = 12 μs). ^{121}Sb NMR spectra were recorded at 14.4 MHz with a 20 kHz sweep width (90° = 10 μs). In all cases, the field was locked using the deuterium signal of the solvent. The temperature was measured by a substitution technique using a Pt resistor, or by using methanol or ethyleneglycol as thermometric solutions [6].

None of the solutions studied contained TMS, since it reacts readily with $SbCl_5$. For ^1H and ^{13}C work the solvent signal was used as an internal shift reference, chemical shifts being quoted with respect to TMS, and temperature effects upon the chemical shift being taken into account where necessary. The high frequency positive convention is adopted throughout, signals occurring to high frequency of the reference being denoted as positive.

Results

Vibrational Study

If the ligand L is assumed to be a point mass, $SbCl_5 \cdot L$ adducts can be assigned to the C_{4v} point group, and have the following vibrational representation:

$$\Gamma_v = 4A_1 + 4E \text{ (R + IR active)}$$
$$= 2B_1 + B_2 \text{ (R active only)}$$

Two A_1 (ν_1 axial and ν_2 symmetric equatorial), one B_1 (ν_5 asymmetric equatorial) and one $E(\nu_8)$ mode correspond to Sb–Cl stretching vibrations, while one $A_1(\nu_3)$ mode represents the Sb–L stretch [7, 8]. Tables I and II list the assignments of these stretching modes for a series of $SbCl_5 \cdot L$ adducts, in the solid state and in solution in CH_2Br_2, respectively, prepared as described in the 'Experimental'. Nearly half of the solid adducts have been the subject of earlier studies, which are acknowledged in Table I. The data have been separated into three classes according to the donor group of the ligand L.

The first class is comprised of the nitriles R–CN (R = $-CH_3$, $-C(CH_3)_3$, $-CH_2I$ and $-SCH_3$). The vibrational study of $SbCl_5 \cdot CH_3CN$ has been the subject of considerable interest in the literature. An X-ray structural determination of this compound [21] shows a linear Cl_{ax}–Sb–N–C arrangement.

The second class considered contains eight Lewis bases with an oxygen donor atom, two of which, DMSO and DMF, have been the subject of detailed vibrational studies [14–16]. These adducts are characterised by a reduction of their symmetry due to the non-linearity of the Cl_{ax}–Sb–L bonds.

The third class is that of the phosphorylated ligands $R_{3-n}R'_nPO$ (R, R' = –Cl, $-OCH_3$, $-N(CH_3)_2$). Their donor strength is particularly sensitive to the inductive effect of the substituents. Indeed the effect is so pronounced that an inversion of the dipole moment of the molecule has been noted between F_3PO and $(CH_3)_3PO$ [22]. Because of the existence of two possible mesomeric electronic configurations, the P=O–Sb linkage is not expected to be linear, and indeed this angle in crystalline $SbCl_5 \cdot POCl_3$ has been shown to be 145° by X-ray measurements [17]. This class of adducts has been the subject of several vibrational studies and the assignments given are based on the $SbCl_5 \cdot POCl_3$ studies undertaken by Gushikem *et al.* [18].

Figure 1 illustrates the vibrational spectra of a typical $SbCl_5 \cdot L$ adduct, that of $SbCl_5 \cdot THF$, in the region of the metal ligand stretching vibrations in the solid and solution states, as well as the region of bending and rocking vibrations for the solid. The spectral assignments of the antimony–chloride vibrational modes are based on the well documented spectra of the $SbCl_5$ adduct with acetonitrile [14], a weak Lewis base, and dimethylsulphoxide [15], a strong Lewis base. The $\nu_1(A_1)SbCl_{ax}$ stretch appears as a strong doublet in both the Raman (344 and 340 cm^{-1}) and the IR (345 and 340 cm^{-1}) spectra of the solid. The splitting of this band is a general feature of the spectra of the solid adducts. Three possibilities have been invoked to explain this fact [15]: an isotopic shift due to the two isotopes of

TABLE I. Sb–Cl and Sb–L Infra-red and Raman Vibrational Frequencies for Several Solid $SbCl_5$•L Adducts[a]

Ligand (L)	Vibrational frequencies (cm^{-1})									
	$\nu_8(E)$		$\nu_1(A_1)$		$\nu_2(A_1)$		$\nu_3(A_1)$		$\nu_5(B_1)$	
	Ra	IR	Ra	IR	Ra	IR	Ra	IR	Ra	IR
CH_3CN [9–12]	371vw	370vs 364vs	350sh	350vs	344vs		223w		295m	
$(CH_3)_3CCN$ [13]	370sh	372vs 367vs	364m 356w	360s 354s	339vs	338sh			297m	
ICH_2CN	378vw	374vs 370vs	366vw	364vs 356sh	343m	342sh		187w	295m	
CH_3SCN	373sh 365m	373s 367s	355m	356vs	337vs	328sh	262vw	266w	294m	
$(CH_3)_2O$	368m 359sh	371vs	352s 348s	348vs 344vs	331vs	332s		475w	295m	
$(CH_3CH_2)_2O$		369vs	349s 344s	348vs 344vs	329vs	331sh		506w	294m	
THF	362vw	367vs	344vs 340vs	345s 340s	330vs	328s		568vs	294m	
$(CH_3)_2CO$	368m 359sh	373vs 364vs	349s 344s	351vs 345vs	331m	331s	434m	434m	294m	
DMSO [14, 15]		365s	351s 344s	355vs 347vs	326vs	329s		502w	289m	
DMF [15, 16]	365vw	360sh	352vs 346sh	354vs 350vs	322vs	325m	435w 425w	439w 424w	290m	
DMA		357vs	348vs 343vs	344sh	326vs	325sh		442w	288m	
TMU	349vw 355vw	350vs 358vs	335vs	339vs		327sh	428vw	430m	282w	286sh
$POCl_3$ [15, 17–19]	372sh	372vs 368vs	364m 351m	353vs 350vs	335vs	335s	385vw	386s	295m	299m
$Cl_2(CH_3O)PO$ [20]	366vw	370vs 366vs	354m 348m	355vs 348vs	337vs	335s	426w	427w	295m	
$Cl(CH_3O)_2PO$ [20]	372vw 366vw	366vs	347vs 344sh	348vs	329vs	330s		434s	295m	
$(CH_3O)_3PO$ [20]	370vw 365vw	371sh 363vs	343vs 341vs	346s 341s	332s	333m	455vw	458vs	294m	
$Cl_2((CH_3)_2N)PO$	371vw 363vw	367vs	355m 349m	356vs 350sh	333vs	332s		423m	296m	
$Cl((CH_3)_2N)_2PO$	365vw	358vs	339vs	340s 335s	328s	326s		446m	286w	288w
$((CH_3)_2N)_3PO$		357s	338vs	338s	326vs	325sh		462m	288m	

[a]Abbreviations for band intensities are given as follows: vs = very strong; s = strong; m = medium; w = weak; vw = very weak; sh = shoulder.

chlorine, ^{35}Cl and ^{37}Cl; the presence of a harmonic or combination mode enhanced by a Fermi resonance; and a factor group splitting. The splitting of the ν_1 mode is not observed in the broader solution band at 357 cm^{-1} (Raman) and 346 cm^{-1} (IR). The $\nu_2(A_1)SbCl_4$ symmetric stretch appears as a strong signal in both the Raman (330 cm^{-1}) and the IR (328 cm^{-1}) spectra of the solid. In solution the ν_2 mode occurs at 329 cm^{-1} in both Raman (polarised) and IR spectra. The $\nu_5(B_1)SbCl_4$ asymmetric stretch,

TABLE II. Sb–Cl Infra-red and Raman Vibrational Frequencies for Several $SbCl_5$•L Adducts in CH_2Br_2[a,b]

Ligand (L)	Vibrational frequencies (cm^{-1})							
	$\nu_8(E)$		$\nu_1(A_1)$		$\nu_2(A_1)$		$\nu_5(B_1)$	
	Ra	IR	Ra	IR	Ra	IR	Ra	IR
CH_3CN	372sh	372vs	360m,p	358sh	339s,p	343w	296m	
$(CH_3)_3CCN$	372sh	372vs	361m,p	361m	336vs	343sh	296m	
ICH_2CN	373sh	372vs	362vw		339s,p	338sh	295m	
CH_3SCN	373sh	371vs	359m,p	356sh	336s,p	336sh	295w	
$(CH_3)_2O$	369sh	369vs	358m,p	346vs	332s,p	332sh	294m	
$(CH_3CH_2)_2O$	368sh	368vs	359m	348m	330s,p	329sh	295sh	
THF	366sh	366vs	357m	346vs	329s,p	329sh	295w	
$(CH_3)_2CO$		369vs	359m,p	346vs	330s,p	332sh	295w	
DMSO		361vs	349m,p	350sh	326s,p		288w	
DMF		362vs	350m,p	348sh	327s,p	324w	291w	
DMA	359sh	361vs	345s,p	347vs	326s,p	327sh	289m	
TMU	362vw	359vs	337vs	343sh	327sh		286w	
$POCl_3$		372vs	353m	352sh	335s,p	337m	295w	
$Cl_2(CH_3O)PO$	370sh	370vs	355m	354sh	334s,p	336w	294m	
$Cl(CH_3O)_2PO$		368vs	350sh	348sh	332s,p	330sh	293m	
$(CH_3O)_3PO$		366vs	346m,p	351sh	330s,p	332w	293w	
$Cl_2((CH_3)_2N)PO$		369vs	352m	352sh	332s,p	334sh	296w	
$Cl((CH_3)_2N)_2PO$		363vs	342m	344vs	328s,p	329sh	289w	
$((CH_3)_2N)_3PO$	362sh	360vs	340s,p	346m	325s,p	326w	287m	

[a]Abbreviations for band intensities are given as follows: vs = very strong, s = strong, m = medium, w = weak, vw = very weak, sh = shoulder, p = polarised. [b]With a 1:2 [$SbCl_5$]/[ligand] ratio, and a total concentration of $SbCl_5$ of between 0.10 and 0.30 m.

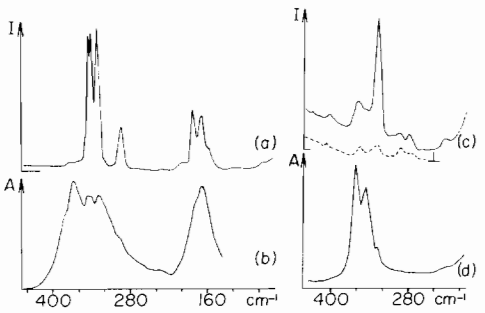

Fig. 1. Raman (a) and infra-red (b) spectra of solid $SbCl_5$•THF, together with Raman (c) and infra-red (d) spectra of an $SbCl_5$•THF solution in CH_2Br_2. The ratio of the concentrations of $SbCl_5$ to THF is 1:2, with an $SbCl_5$ concentration of 0.10 m.

which is Raman active only, is noted at 294 cm^{-1} in the solid and at 295 cm^{-1} in solution. The $\nu_8(E)$-$SbCl_4$ mode is very weak in the Raman spectra, at 362 cm^{-1} in the solid and at 366 cm^{-1} in solution, and very strong in the IR spectra, at 367 cm^{-1} and 366 cm^{-1}, respectively. The very strong IR signal observed in the solid at 568 cm^{-1} (not shown in Fig. 1) may be assigned to the $\nu_3(A_1)$Sb–O stretch by comparison with values reported in the literature for the same class of ligands: it is noted at around 500 cm^{-1} (Raman and IR) for adducts with DMSO [14, 15] and at 422 to 440 cm^{-1} (Raman) and 422–438 cm^{-1} (IR) for those with DMF [15].

Tentative assignments of the bending and rocking modes, measured for the solid alone, may be made as follows. The $\nu_4(A_1)SbCl_4$ out of plane deformation is observed as a strong signal at 170 cm^{-1} in the Raman spectrum, and as a doublet at 170 cm^{-1} and 166 cm^{-1} in the IR. The strong signal at 182 cm^{-1} in the Raman spectrum is assigned to the asymmetric $\nu_7(B_1)SbCl_4$ out of plane deformation. The two $\nu_9(E)Cl–SbCl_4$ and $\nu_{10}(E)O–SbCl_4$ wagging modes are noted at 156 cm^{-1} and at 203 cm^{-1} in the Raman spectrum, respectively. The very low intensity Raman band in the 120–125 cm^{-1} region may be due to the $\nu_{11}(E)SbCl_4$ in-plane deformation. The expected $\nu_6(B_1)SbCl_4$ out-of-plane deformation could not be assigned. The weak signals at 278 cm^{-1} and 280 cm^{-1} in the Raman spectra of the solid and the solution, respectively, are assigned to internal vibrations of the THF molecule, since, in the case of the latter, its intensity is proportional to the concentration of THF in solution.

Finally, it should be noted that spectra of the solids yield sharper lines than spectra of the solutions, often exhibiting splittings not apparent in the solution spectra. The relative intensities of the lines in the spectra of the solids may differ considerably from

one adduct to the next, whereas the solution spectra of the various adducts are generally comparable, a fact which greatly facilitates the assignments.

Auto-ionisation in $SbCl_5$·L Solutions

The auto-ionisation equilibrium (2) has been clearly shown to exist by vibrational [12] and NMR [23] studies. The three main vibrations [8] of centro-

$$2SbCl_5 \cdot L \rightleftharpoons SbCl_4 \cdot 2L^+ + SbCl_6^- \quad (2)$$

symmetric $SbCl_6^-$, the IR active $\nu_3(F_{1u})$ at 353 cm^{-1}, the Raman active $\nu_1(A_{1g})$ at 330 cm^{-1} and $\nu_2(E_g)$ at 282 cm^{-1}, occur in the region of the $\nu_1(A_1)$, $\nu_2(A_1)$ and $\nu_5(B_1)$ vibrations of the $SbCl_5$·L adducts, respectively. For this reason, even in favourable cases, detection of small amounts (<5%) of the hexachloroantimonate(V) species in the presence of the adducts is impossible. Therefore no evidence of this species has been found in the Raman and the IR solution spectra of the adducts studied in the preceding section.

Antimony-121 NMR has been shown to be a sensitive technique in tracing small concentrations of the highly symmetric $SbCl_6^-$ ion [23]. Solutions of $[SbCl_6](CH_3CH_2)_4N$ were used as a standard for concentration determination, the NMR signal being detectable at concentrations of less that 10^{-3} m [24]. Using this technique we have observed approximately 7% $SbCl_6^-$ in nitromethane solutions (ϵ = 35.9) 0.1 m in $SbCl_5$·$((CH_3)_2N)_3PO$ with an excess of the strong donor $((CH_3)_2N)_3PO$ (1:2). This value falls to about 3% in the less polar solvent dichloromethane (ϵ = 9.1). Similar values have been observed for solutions with two other strong donors, DMSO and TMU. However, as soon as the donor strength of the ligand L decreases, for example with CH_3CN, the $SbCl_6^-$ species can no longer be detected (<1%) even in the highly polar solvent nitromethane. Generally, the extent of auto-ionisation increases with the polarity of the solvent and the donor strength of the ligand. Typically for 0.1 m $SbCl_5$·L solutions in CD_2Cl_2, such as those used in our NMR studies, the quantity of ionic species is less than 1%, except for the strongest donors where it can reach 3%.

NMR Data

All $SbCl_5$·L solutions investigated for this work contained an equimolar excess of ligand L. The adducts display characteristic NMR kinetic windows depending on their lability. To allow a kinetic study over the greatest temperature range possible, appropriate inert solvents were chosen. Under conditions of blocked chemical exchange only two signals pertaining to the ligand could be observed, that of the bound ligand in $SbCl_5$·L and that of the free ligand L. The $[SbCl_5]$/[coordinated L] ratio in the adduct has been verified on the basis of the known concentrations of $SbCl_5$ and ligand, and the integration of both ligand NMR signals. In all cases this ratio was found to be 1:1 within experimental error. This ratio and the absence of any other ligand L NMR signal are taken as further evidence that the concentration of ionic species is negligible under the conditions used.

TABLE III. Coupling Constants (J), Chemical Shifts (δ-($SbCl_5$·L)) and Chemical Shift Differences ($\Delta\delta = \delta(SbCl_5 \cdot L) - \delta(L)$) for $SbCl_5$·L Adducts[a], Referenced to TMS[b], in CH_2Cl_2 at 298 K Except where Stated

Ligand (L)	δ ±0.01 (ppm)	$\Delta\delta$ ±0.01 (ppm)	J (Hz) $SbCl_5$·L	L
^1H NMR at 60 MHz				
CH_3CN[e]	2.79	0.66		
$(CH_3)_3CCN$[f]	1.64	0.25		
ICH_2CN[e]	4.12	0.48		
CH_3SCN[e]	2.99	0.34		
$(CH_3)_2O$[e]	4.27	0.76		
$(CH_3CH_2)_2O$[c,g]–(CH_2)–	4.58	1.22		
$(CH_3CH_2)_2O$[c,g]–(CH_3)	1.48	0.34		
$(CH_3)_2CO$[g]	2.95	0.68		
DMF[d]–H	8.58	0.57		
DMF[d]–$(CH_3)_t$	3.43	0.44		
DMF[d]–$(CH_3)_c$	3.30	0.40		
DMA[d]–(CH_3)	2.71	0.57		
DMA[d]–$(CH_3)_t$	3.44	0.38		
DMA[d]–$(CH_3)_c$	3.35	0.38		
TMU[d]	3.22	0.41		
DMSO[d]	3.14	0.50		
$Cl_2(CH_3O)PO$[e,i]	4.38	0.32	17.6	17.5
$Cl(CH_3O)_2PO$[c,h,i]	4.32	0.34	14.6	13.9
$(CH_3O)_3PO$[d,i]	4.13	0.35	11.9	10.9
$Cl_2((CH_3)_2N)PO$[e,i]	3.09	0.20	16.6	15.7
$Cl((CH_3)_2N)_2PO$[d,i]	2.93	0.20	13.9	12.8
$((CH_3)_2N)_3PO$[d,i]	2.80	0.20	10.4	9.3
^{13}C NMR at 90.6 MHz				
$(CH_3O)_3PO$[f,j]	58.00	3.26	7.0	7.0
THF[f]–C_α–	72.27	4.62		
THF[f]–C_β–	24.88	−0.50		

[a]All solutions had a $[SbCl_5]$/[ligand] ratio of 1:2, and a total $SbCl_5$ concentration of between 0.10 and 0.30 m. [b]The solvent resonance was taken as an internal reference, δ values being obtained by referring this to the resonance of TMS in a 1% solution in the appropriate solvent, temperature effects having been taken into account. [c]In $CHCl_3$. [d]In $(CHCl_2)_2$. [e]At 193 K. [f]At 214 K. [g]At 243 K. [h]At 264 K. [i]$^3J_{^1H-^{31}P}$. [j]$^2J_{^{13}C-^{31}P}$.

Table III lists the chemical shifts of the ligand in the $SbCl_5$·L adducts, and the chemical shift difference between this and the corresponding free ligand. In ^1H NMR the coordination of L always induces a high frequency shift, indicating a reduction in nuclear shielding. The extent of this shielding, due to charge transfer from the ligand L to the Lewis acid $SbCl_5$, is similar to that observed previously in

$MCl_5 \cdot L$ (M = Nb, Ta) adducts [25, 26]. We also recorded the $^{13}C\{^1H\}$ NMR spectra in the case of $(CH_3)O)_3PO$ and THF. For the β-carbon of the latter an unexpected low frequency shift of 0.50 ppm due to coordination has been noted. Where appropriate the magnitude of the phosphorous-31 coupling constants are given in Table III, being slightly greater for the bound ligand in all cases.

Relative Stability of the Adducts

The quantitative reaction between $SbCl_5$ and the Lewis bases L to form the $SbCl_5 \cdot L$ adducts does not allow a straightforward determination of their very high stability constants. However, NMR can be used to establish the relative stability constant of the adducts by investigating the following competitive equilibrium:

$$SbCl_5 \cdot L_b + L_a \rightleftharpoons SbCl_5 \cdot L_a + L_b \quad (3)$$

$$K_{a,b} = [SbCl_5 \cdot L_a][L_b]/[L_a][SbCl_5 \cdot L_b] \quad (4)$$

in which $K_{a,b}$ is the relative stability constant of the adduct formed with ligand L_a with respect to that formed with L_b. All these constants were determined under blocked ligand exchange conditions. Whenever possible the relative intensities of the NMR signals of the four species in equilibrium were directly obtained by integration and inserted into eqn. (4), as illustrated in Fig. 2. In situations in which this procedure was hampered by a poor signal-to-noise ratio and/or by spectral overlap, an indirect method was employed, taking into account the initial reactant concentrations, or by integrating with respect to a quantitative reference, usually the ^{13}C satellite signal of the solvent [26, 28]. ^1H NMR was used in all cases except that of $K_{(CH_3O)_3PO,THF}$ where the results were derived from $^{13}C\{^1H\}$ NMR, in view of the complexity of the ^1H NMR spectrum.

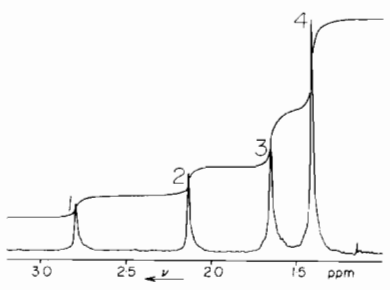

Fig. 2. A 60 MHz ^1H NMR spectrum of a solution used in the determination of the relative stability constant for the equilibrium:

$SbCl_5 \cdot (CH_3)_3CCN + CH_3CN \rightleftharpoons SbCl_5 \cdot CH_3CN + (CH_3)_3CCN$

for which $K_{CH_3CN,(CH_3)_3CCN} = 1.5$. The concentrations are approximately 0.05 m in $SbCl_5$ and 0.07 m in each ligand, with CD_2Cl_2 as solvent. Peaks 1 to 4 are assigned as follows: 1 arises from $SbCl_5 \cdot CH_3CN$, 2 from CH_3CN, 3 from $SbCl_5 \cdot (CH_3)_3CCN$ and 4 is due to $(CH_3)_3CCN$.

As far as the conditions allowed, we have verified some values of $K_{a,b}$ by means of a cycle, measuring $K_{a,c}$ and $K_{c,b}$, for which the product $K_{a,b}'$ should be equal to $K_{a,b}$. The values retained for the stability constants $K_{a,b}''$ have been obtained by taking into account both constants $K_{a,b}$ and $K_{a,b}'$. The results are given in Table IV and Fig. 3.

Discussion

Extensive calorimetric measurements on the interactions of oxygen and nitrogen containing solvent molecules with antimony(V) pentachloride as reference acceptor in dichloromethane, according to eqn. (5),

$$SbCl_5 + L \rightleftharpoons SbCl_5 \cdot L \quad (5)$$

were published by Gutmann [5]. He introduced the concept of 'donor-number', defined as 'the numerical quantity of $-\Delta H_{SbCl_5 \cdot L}$(kcal mol^{-1})' and which may be interpreted as reflecting a molecular property of the solvent. For this equilibrium he obtained some stability constants, $K_{SbCl_5 \cdot L}$, from spectrophotometric measurements. In this study we report the relative stability constants of a large series of $SbCl_5 \cdot L$ adducts (Table IV). For the few cases where the comparison is possible, the results from both techniques are in agreement. The linear relationship illustrated in Fig. 4 between the donor number, DN_{SbCl_5}, and the relative free energy of reaction, $\Delta\Delta G$, shows that the entropic contributions are similar for all donor L/acceptor $SbCl_5$ reactions under consideration except for hexamethylphosphortriamide. It appears that $SbCl_5 \cdot ((CH_3)_2N)_3PO$ is somewhat entropy-destabilised with respect to the other adducts.

The stability constants of $SbCl_5 \cdot L$ adducts are compared in Fig. 3 with those of $NbCl_5 \cdot L$ and $TaCl_5 \cdot L$ published previously [25–29]. The small cations Sb^{5+}, Nb^{5+} and Ta^{5+} having an ionic radius of between 0.60 and 0.64 Å and a high charge have a predictable hard acid behaviour. However, it has been shown [26] that the Lewis acids $NbCl_5$ and $TaCl_5$ have a soft behaviour, forming more stable adducts with $(CH_3)_2Te$, $(CH_3)_2Se$ and $(CH_3)_2S$ than with $(CH_3)_2O$ and $(CH_3CH_2)_2O$. This has been attributed to the symbiotic effect of the chlorides which confer a soft character to the Lewis acid. On the basis of a high Ca/Ea ratio, Drago [30] classifies $SbCl_5$ among the soft acids. The observed decomposition of $SbCl_5$ in the presence of soft bases, for example dimethylsulfide and dimethylselenide, may be due to a strong interaction between antimony and the Lewis base.

The stability of $SbCl_5$ adducts with dimethylether and diethylether is greater than that with the nitriles. This contrasts with the behaviour of the

TABLE IV. Relative Stability Constants $K_{a,b}$ for the Adducts $SbCl_5$•L[a] in CH_2Cl_2, According to the Equilibrium: $SbCl_5$•L_b + L_a ⇌ $SbCl_5$•L_a + L_b

La	L_b	T(K)	$K_{a,b}$	L_c	$K_{a,b}'$[b]	log $K_{a,b}''$[c]
$((CH_3)_2N)_3PO$	DMSO	298	6.8 ± 1.4			0.83
	DMF	298	83 ± 16	DMSO	71 ± 28	1.85
DMSO	DMF	298	10.5 ± 2.1			1.02
	TMU	298	23 ± 5	DMF	22 ± 9	1.34
DMF	TMU	298	2.1 ± 0.4			0.32
	DMA	298	6.0 ± 0.3	TMU	6.3 ± 2.5	0.80
TMU	DMA	298	3.0 ± 0.6			0.48
	$Cl((CH_3)_2N)_2PO$	213	3.9 ± 0.3			0.59
$Cl((CH_3)_2N)_2PO$	$(CH_3)_3PO$	213	6.5 ± 1.0			0.81
$(CH_3O)_3PO$	THF	213	680 ± 250			2.83
THF	$Cl(CH_3O)_2PO$	193	1.6 ± 0.2			0.20
$Cl(CH_3O)_2PO$	$Cl_2((CH_3)_2N)PO$	193	10.9 ± 3.0			1.04
	$(CH_3CH_2)_2O$	193	50 ± 5	$Cl_2((CH_3)_2N)PO$	57 ± 24	1.76
$Cl_2((CH_3)_2N)PO$	$(CH_3)_2O$	203	1.5 ± 0.3			0.18
	$(CH_3CH_2)_2O$	203	5.2 ± 0.8			0.72
$(CH_3)_2O$	$Cl_2(CH_3O)PO$	193	27.0 ± 5.5			1.43
	CH_3CN	193	111 ± 6	$Cl_2(CH_3O)PO$	180 ± 76	2.27
$(CH_3CH_2)_2O$	$(CH_3)_2CO$	203	1.5 ± 0.2			0.18
$Cl_2(CH_3O)PO$	CH_3CN	193	6.8 ± 1.0			0.84
	CH_3SCN	193	34 ± 2	CH_3CN	36 ± 11	1.51
CH_3CN	$(CH_3)_3CCN$	193	1.5 ± 0.4			0.20
	CH_3SCN	193	5.3 ± 0.8	$(CH_3)_3CCN$	4.1 ± 2.0	0.67
$(CH_3)_3CCN$	CH_3SCN	193	2.7 ± 0.6			0.47
CH_3SCN	ICH_2CN	175	43 ± 6			1.63

[a] $[SbCl_5]_t$ = 0.05 m and $[L_a]_t + [L_b]_t$ = 0.10 m to 0.30 m. [b] $K_{a,b}' = K_{a,c} \times K_{c,b}$. [c] $K_{a,b}''$ is the definitive value of $K_{a,b}$ adopted, taking into account the values of $K_{a,b}$ and $K_{a,b}'$.

corresponding $NbCl_5$ and $TaCl_5$ adducts. We also note that for niobium and tantalum the adducts with diethylether are less stable than those with dimethylether, as expected on steric grounds. This difference in stability is much less pronounced for the analogous antimony adducts. This can be understood by comparing the metal–chloride bond lengths in the two isomorphous MX_5•$POCl_3$ adducts of niobium and antimony which are, respectively [17]: M–Cl_{eq} = 2.31 and 2.34 Å, M–Cl_{ax} = 2.25 and 2.35 Å. The consequent reduction of steric hindrance in the antimony adducts accounts for the smaller stability difference between both ethers, and possibly also the greater stability of the ethers with respect to the nitriles. Moreover, the greater stability of the $SbCl_5$•THF adduct with respect to that of dialkylethers is due to smaller steric effects (C–O–C angles: 106.2° in THF [31] and 111.8° in $(CH_3CH_2)_2O$ [32]) and the possibility of an increase in the donor strength due to cyclisation.

Beside the steric effects, the other main factor governing the stability of these adducts is that of the inductive effect of the various substituents on the ligand. This is particularly apparent with the family of phosphorylated ligands: with the –I effect of the chloride, an electron attractor, and the +M effect of the electron donating groups CH_3O and $(CH_3)_2N$, the latter being the strongest electron donor. The resulting variation in the electron density of the ≡PO group, and consequent donor strength, explains the following observed stability series: $Cl_2(CH_3O)$-PO < $Cl_2((CH_3)_2N)PO$ < $Cl(CH_3O)_2PO$ < $(CH_3$-$O)_3PO$ < $Cl((CH_3)_2N)_2PO$ < $((CH_3)_2N)_3PO$. A similar effect is apparent with the nitriles [29]. The three main antimony–chloride stretching modes of the series of $SbCl_5$•L adducts in solution may be correlated with their relative stability constants, as determined by NMR. On the whole, an increase in adduct stability, that is in the strength of the Sb–L bond, results in an increased negative charge on the metal atom. This in turn will cause a weakening of the Sb–Cl bonds, which is reflected in the decrease of the $\nu_1(A_1)SbCl_{ax}$, $\nu_2(A_1)SbCl_4$ and $\nu_8(E)SbCl_4$ stretching frequencies as shown in Fig. 5. This correlation holds best for the $SbCl_4$ equatorial stretch, but is less satisfactory for the Sb–Cl axial stretch, since this will not only be affected by the Sb–L bond strength but also by the mass of the ligand and the angular properties of the Sb–L bond. As expected, the effect of L on the amplitude of the frequency shift is more pronounced for the $\nu_1(A_1)$ stretch ($\Delta\nu$ = 25 cm^{-1}) involving the bond *trans* to L than for the equatorial $\nu_2(A_1)$ ($\Delta\nu$ = 14 cm^{-1}) and $\nu_8(E)$ ($\Delta\nu$ = 13 cm^{-1}) vibrations. The Sb–L vibration-

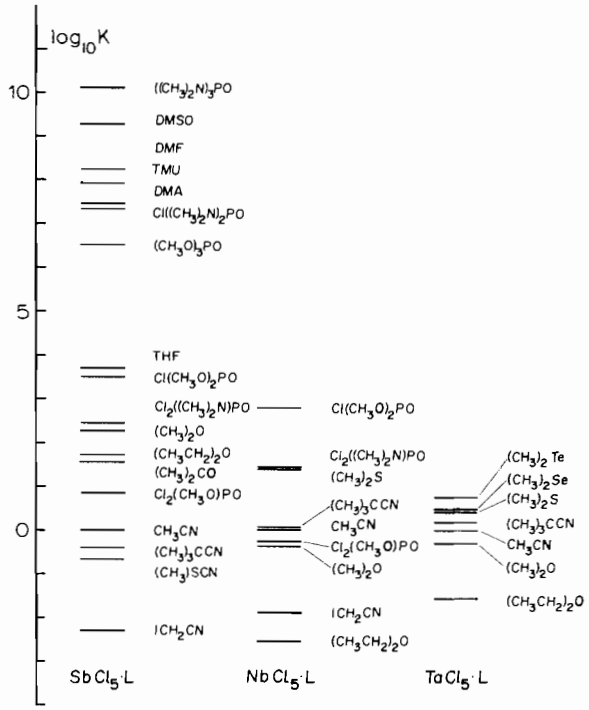

Fig. 3. Relative stabilities of MCl_5 adducts, as determined by NMR. For M = Nb and Ta, the results were obtained at 213 K in 0.10 m $CDCl_3$ solutions [26, 27]. For M = Sb, the measurements were made at *ca.* 193 K in CD_2Cl_2 for the series L = ICH_2CN to $Cl((CH_3)_2N)_2PO$, at 213 K for L = DMA and at 298 K for the remaining adducts. The total $SbCl_5$•L concentration is 0.05 m. The stabilities of the MCl_5•CH_3CN adducts have arbitrarily been set to the same value in order to allow a direct comparison between the three Lewis acids. The stabilities increase from bottom to top.

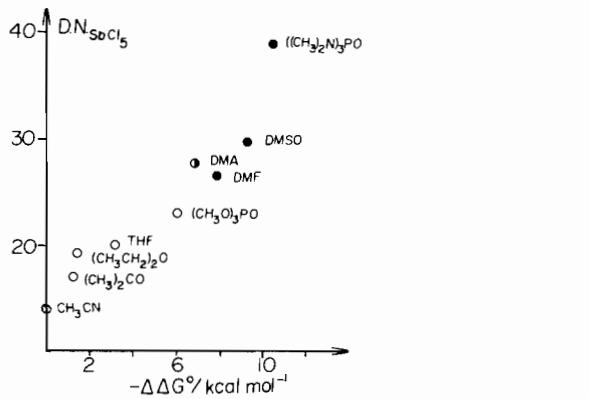

Fig. 4. Donor number $DN = -\Delta H_{SbCl_5 \cdot L}$ as a function of relative free energy of formation $\Delta\Delta G^\circ$ of $SbCl_5$•L adducts derived from stability constants measured at *ca.* 193 K (○), at 213 K (◑) and 298 K (●). The $\Delta\Delta G^\circ$ value for $SbCl_5$•CH_3CN has been arbitrarily set to zero.

al frequency, $\nu_3(A_1)$ (see Table II), is strongly coupled to ligand vibration modes and shows no direct correlation with adduct stability.

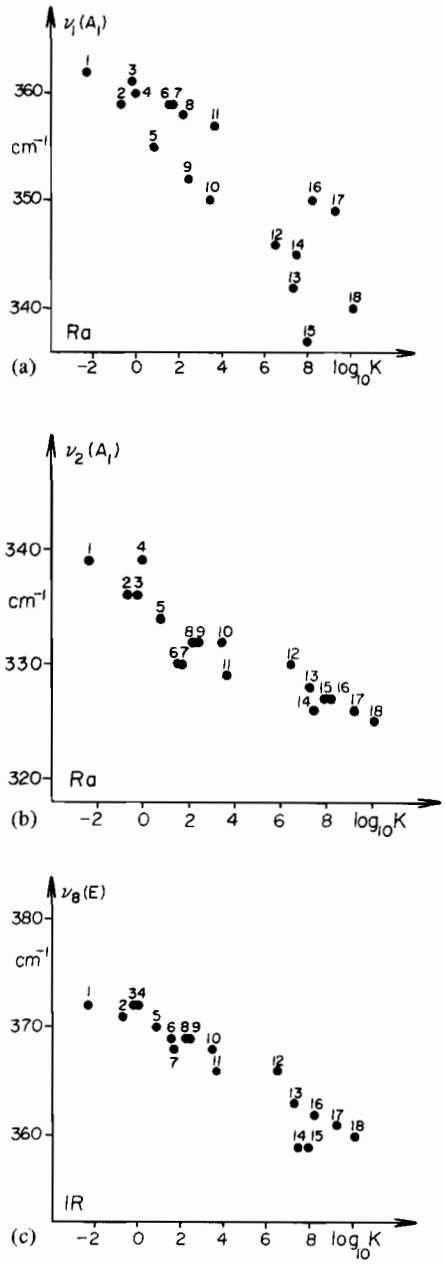

Fig. 5. Antimony–chlorine stretching frequencies of $SbCl_5$•L adducts as a function of their relative stability constants, as determined by NMR spectroscopy. (a) $\nu_1(A_1)$ vibration measured from the Raman solution data. (b) $\nu_2(A_1)$ vibration, from Raman solution data. (c) $\nu_8(E)$ vibration, using IR solution data. Numbered points correspond to the following adducts in all cases: 1 = ICH_2CN; 2 = $(CH_3)SCN$; 3 = $(CH_3)_3CCN$; 4 = CH_3CN; 5 = $Cl_2(CH_3O)PO$; 6 = $(CH_3)_2CO$; 7 = $(CH_3CH_2)_2O$; 8 = $(CH_3)_2O$; 9 = $Cl_2((CH_3)_2N)PO$; 10 = $Cl(CH_3O)_2PO$; 11 = THF; 12 = $(CH_3O)_3PO$; 13 = $Cl((CH_3)_2N)_2PO$; 14 = DMA; 15 = TMU; 16 = DMF; 17 = DMSO; 18 = $((CH_3)_2N)_3PO$.

In conclusion, vibrational and nuclear magnetic resonance spectroscopy show that the structure of $SbCl_5$•L adducts (L = RCN, $R_{3-n}R_n'PO$ and various

oxygen donors) in inert solvents belongs to the C_{4v} point group, and that the extent of auto-ionisation is negligible for the ligands studied. The relative stability constants of these adducts have been measured and provide the necessary background for the mechanistic study detailed in the following paper.

Acknowledgement

The work was financially supported by the Swiss National Science Foundation (Grant No 2.024-0.83).

References

1 D. W. Margerum, G. R. Cayley, D. C. Wheatherburn and G. K. Pagenkopf, in A. E. Martell (ed.), 'Coordination Chemistry', Vol. 2, Am. Chem. Soc., Washington D.C., 1978, pp. 1–220.
2 H. Vanni and A. E. Merbach, *Inorg. Chem., 18*, 1758 (1979).
3 S. J. Ruzicka, C. M. P. Favez and A. E. Merbach, *Inorg. Chim. Acta, 23*, 239 (1977).
4 A. E. Merbach, *Pure Appl. Chem., 54*, 1479 (1982).
5 V. Gutmann, 'Coordination Chemistry in Non-Aqueous Solutions', Springer Verlag, Vienna, 1968.
6 C. Ammann, P. Meier and A. E. Merbach, *J. Magn. Reson., 46*, 329 (1982).
7 C. J. Adams and A. J. Downs, *J. Inorg. Nucl. Chem., 34*, 1829 (1972).
8 K. Nakamoto, 'Infrared and Raman Spectra of Inorganic and Coordination Compounds', Wiley, New York, 1978.
9 M. Burgard and J. MacCordick, *Inorg. Nucl. Chem. Lett., 6*, 599 (1970).
10 D. M. Byler and D. F. Schriver, *Inorg. Chem., 13*, 2697 (1974).
11 I. R. Beattie and M. Webster, *J. Chem. Soc., B, 2*, 38 (1963).
12 C. D. Schmulbach and I. Y. Ahmed, *J. Chem. Soc. A*, 3009 (1968).
13 M. Masson, J. A. Payne and M. J. F. Leroy, *Spectrochim. Acta, Part A, 33*, 37 (1977).
14 M. Burgard and M. J. F. Leroy, *J. Mol Struct., 20*, 153 (1974).
15 M. Burgard, J. P. Brunette and M. J. F. Leroy, *Inorg. Chem., 15*, 1225 (1976).
16 K. J. Ruoff and A. Schmidt, *Spectrochim. Acta, Part A, 32*, 1165 (1976).
17 C.-I. Bränden and I. Lindqvist, *Acta Chem. Scand., 17*, 353 (1963).
18 Y. Gushikem, O. L. Alves, Y. Hase and Y. Kawano, *J. Coord. Chem., 6*, 179 (1977).
19 C. C. Smitskamp, K. Olie and H. Gerding, *Z. Anorg. Allg. Chem., 359*, 318 (1968).
20 K. D. Pressl and A. Schmidt, *Z. Anorg. Allg. Chem., 422*, 266 (1976).
21 H. Binas, *Z. Anorg. Allg. Chem., 352*, 271 (1967).
22 E. L. Wagner, *J. Am. Chem. Soc., 85*, 161 (1963).
23 P. Stilbs and G. Olfsson, *Acta Chem. Scand., Ser. A, 28*, 647 (1974).
24 R. Good, D. R. Zbinden, J.-E. Kessler and A. E. Merbach, *Inorg. Chim. Acta, 28*, 2155 (1978).
25 A. E. Merbach and J.-C. G. Bünzli, *Helv. Chim. Acta, 54*, 2543 (1971).
26 R. Good and A. E. Merbach, *Helv. Chim. Acta, 57*, 1192 (1974).
27 C. M. P. Favez, H. Rollier and A. E. Merbach, *Helv. Chim. Acta, 59*, 2383 (1976).
28 A. E. Merbach and J.-C. G. Bünzli, *Helv. Chim. Acta, 54*, 2536 (1971).
29 A. E. Merbach and J.-C. G. Bünzli, *Helv. Chim. Acta, 55*, 580 (1972).
30 K. F. Purcell and J. C. Kotz, in 'Inorganic Chemistry', Saunders, Philadelphia, 1977, pp. 218–224.
31 R. Fourne, *Acta Crystallogr., Sect. B, 28*, 2924 (1972).
32 D. André, R. Fourne and K. Zechmeister, *Acta Crystallogra., Sect. B, 28*, 2389 (1972).